Supporting Information

Chemical Synthesis of Zr-/Ce-/Sm-containing Intermetallic Compounds Catalyzing $NaBH_4$-assisted Hydrogenation of 4-Nitrophenol

Yasukazu Kobayashi *[a], Hiroshi Mizoguchi [b], Koharu Yamamoto [c], and Ryo Shoji [c]

a. *Renewable Energy Research Centre, National Institute of Advanced Industrial Science and Technology, 2-2-9 Machiikedai, Koriyama, Fukushima 963-0298, Japan.* * Corresponding author, E-mail: yasu-kobayashi@aist.go.jp*

b. *Research Center for Materials Nanoarchitectonics (MANA), National Institute for Materials Science (NIMS) Tsukuba, Ibaraki 305-0044. Japan.*

c. *Department of Chemical Science and Engineering, National Institute of Technology, Tokyo College, 1220-2 Kunugida, Hachioji, Tokyo 193-0997, Japan.*

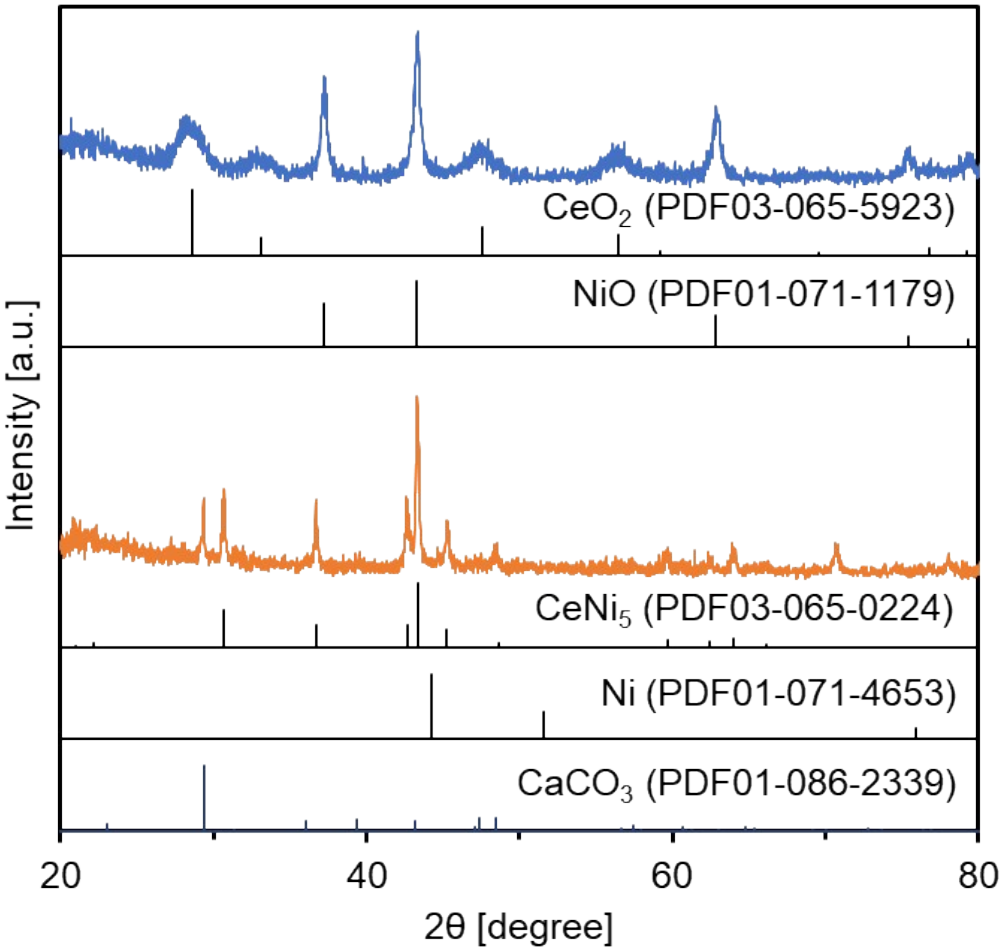

Fig. S1 XRD patterns for the oxide precursor (blue) and the reduced sample (orange) of $CeNi_5$.

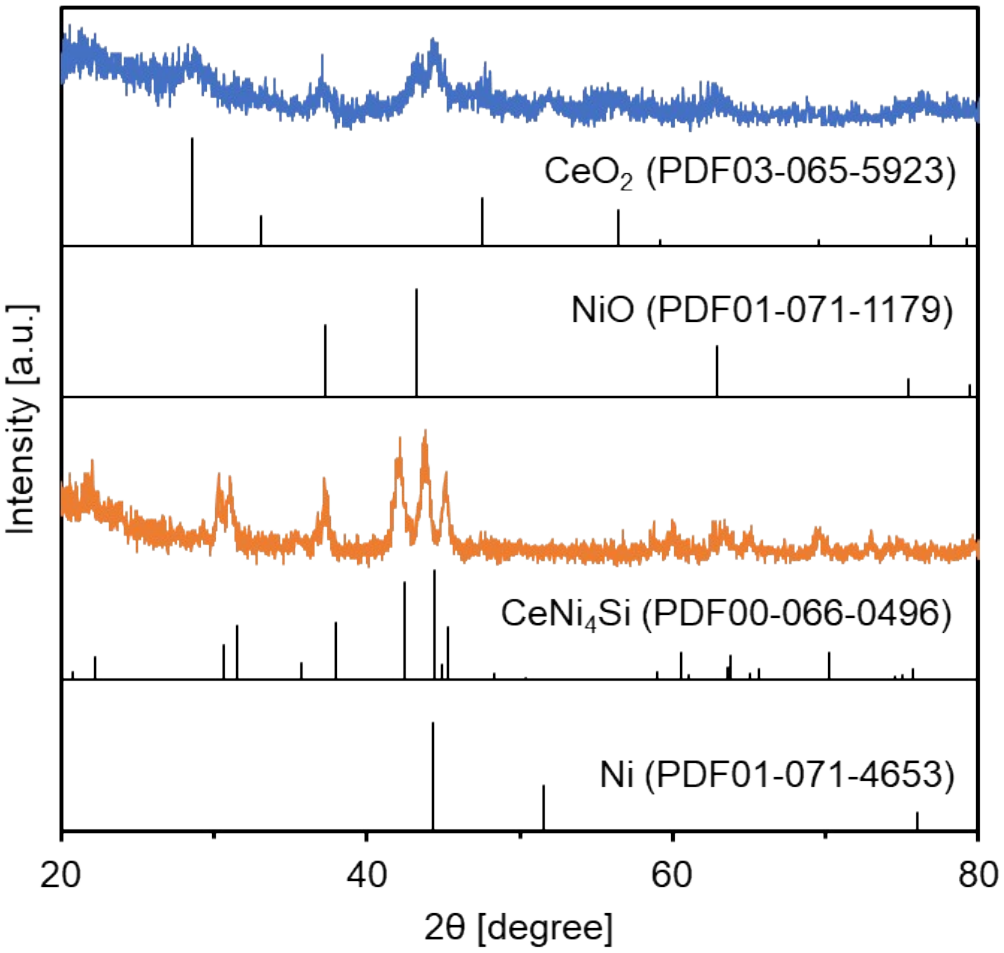

Fig. S2 XRD patterns for the oxide precursor (blue) and the reduced sample (orange) of $CeNi_4Si$.

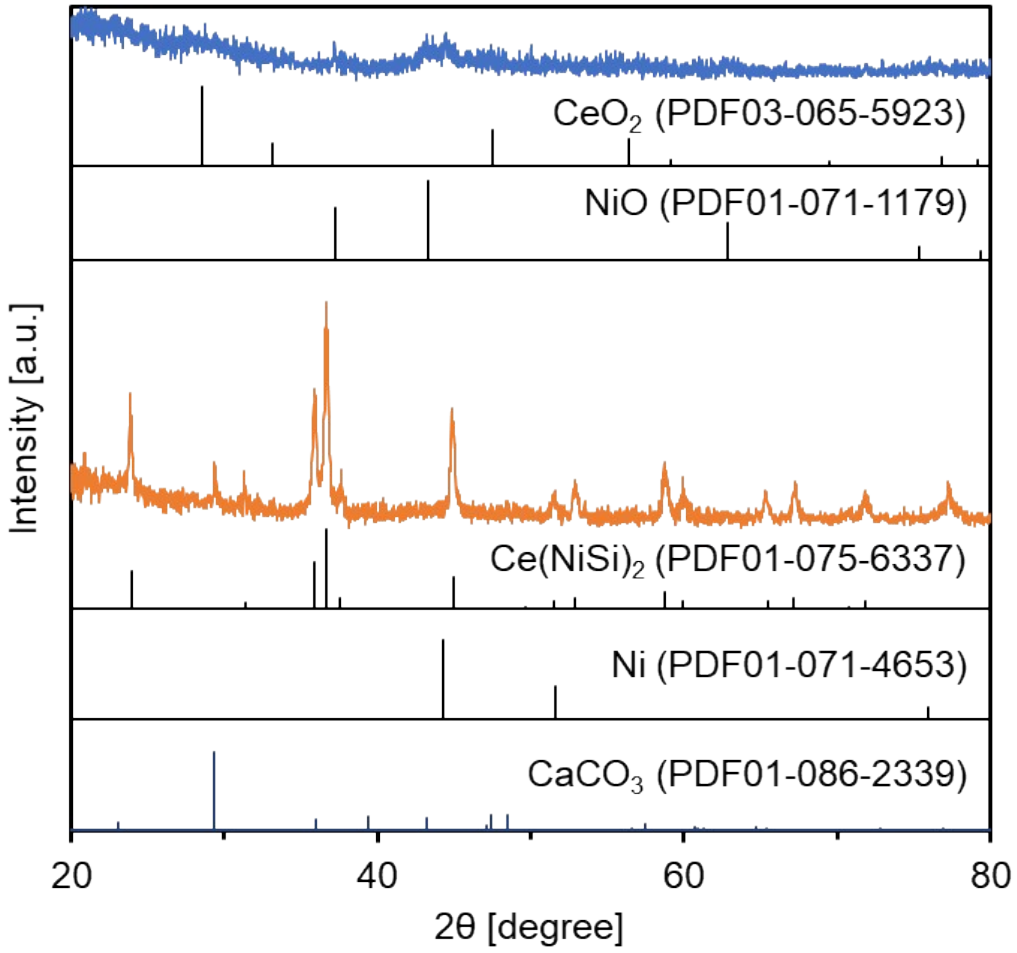

Fig. S3 XRD patterns for the oxide precursor (blue) and the reduced sample (orange) of $Ce(SiNi)_2$.

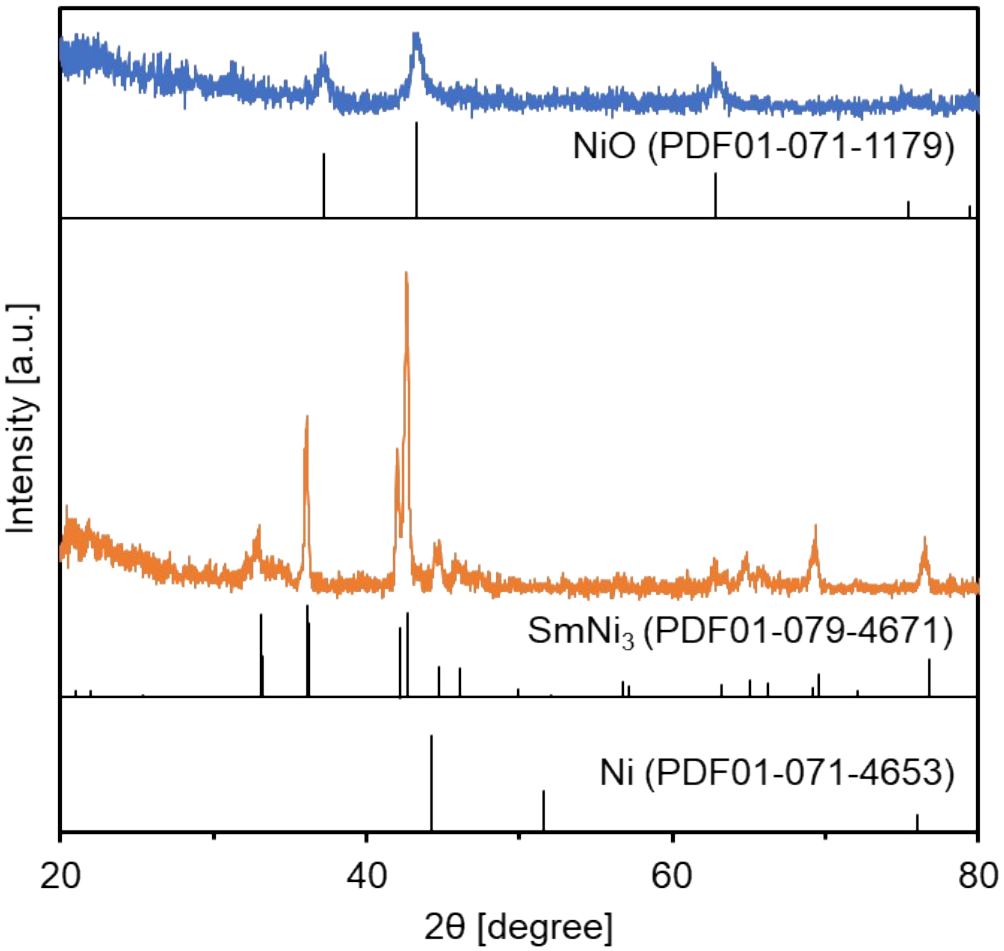

Fig. S4 XRD patterns for the oxide precursor (blue) and the reduced sample (orange) of $SmNi_3$.

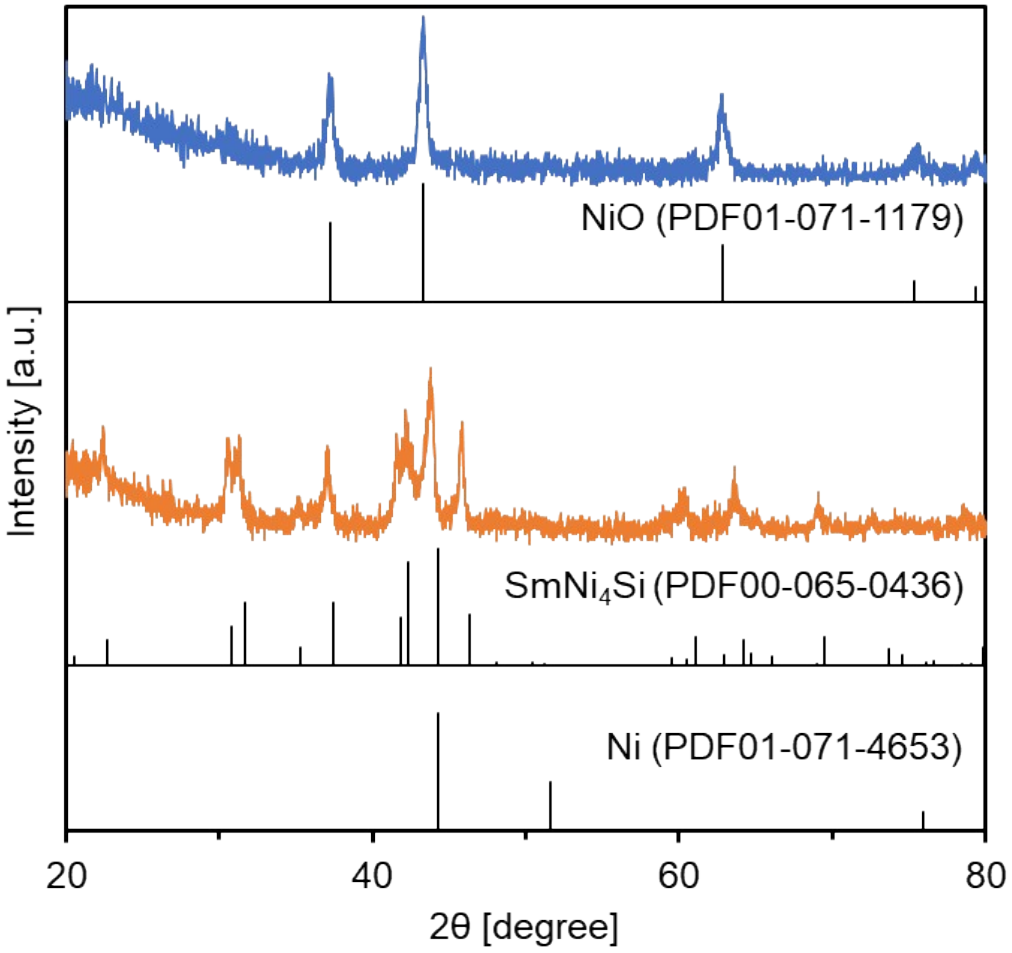

Fig. S5 XRD patterns for the oxide precursor (blue) and the reduced sample (orange) of $SmNi_4Si$.

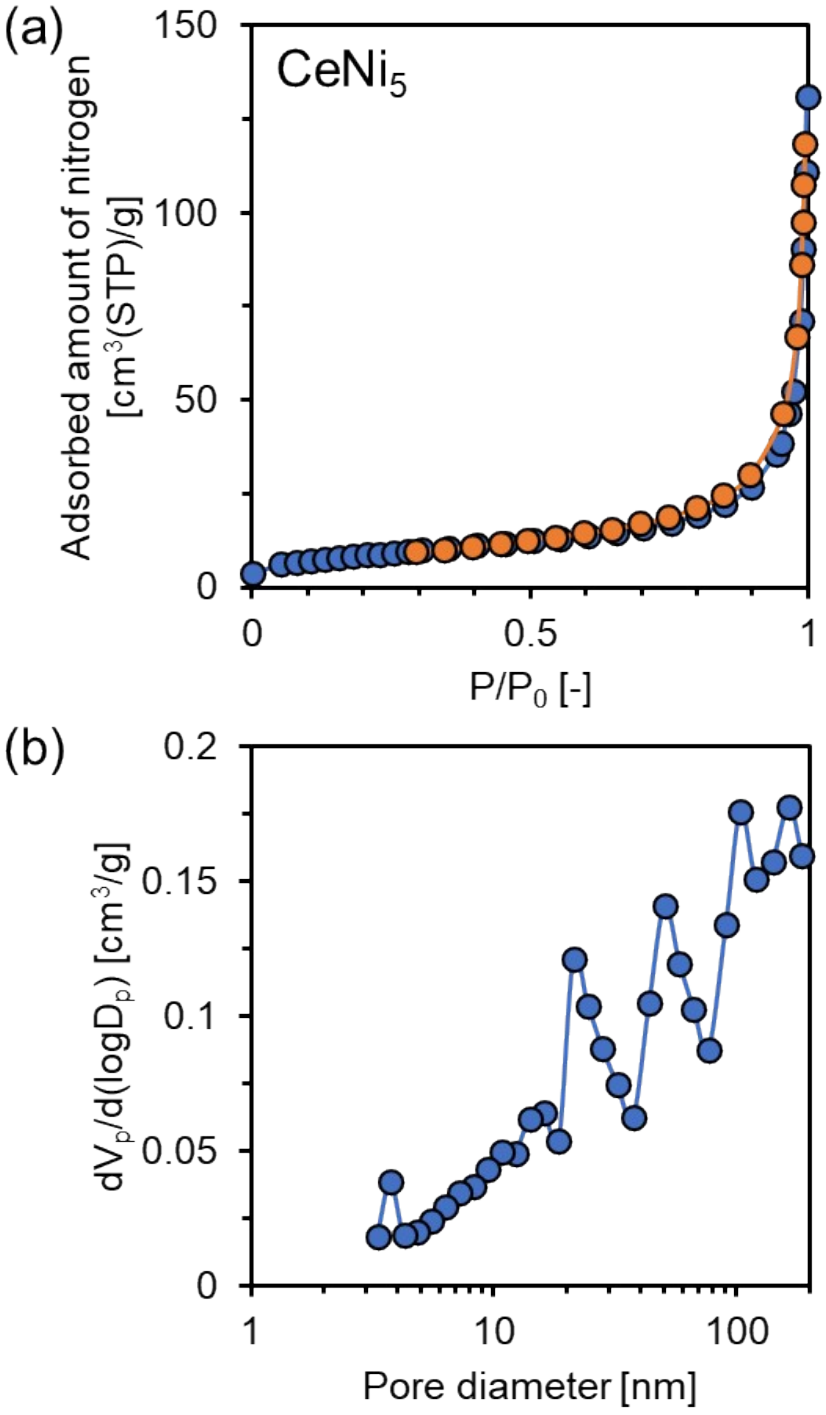

Fig. S6 (a) Adsorption (blue) and desorption (orange) isotherms of nitrogen, and (b) the corresponding pore size distribution for $CeNi_5$.

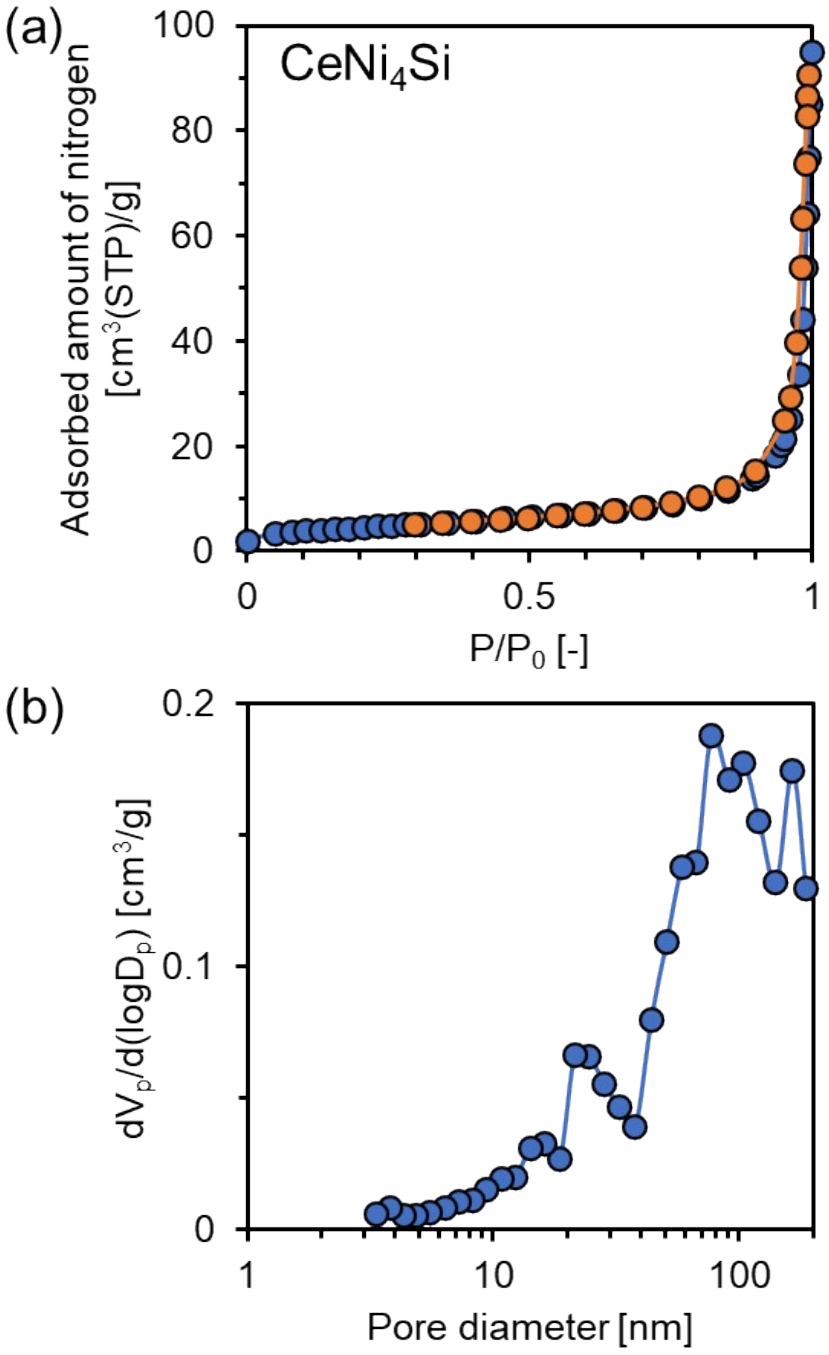

Fig. S7 (a) Adsorption (blue) and desorption (orange) isotherms of nitrogen, and (b) the corresponding pore size distribution for $CeNi_4Si$.

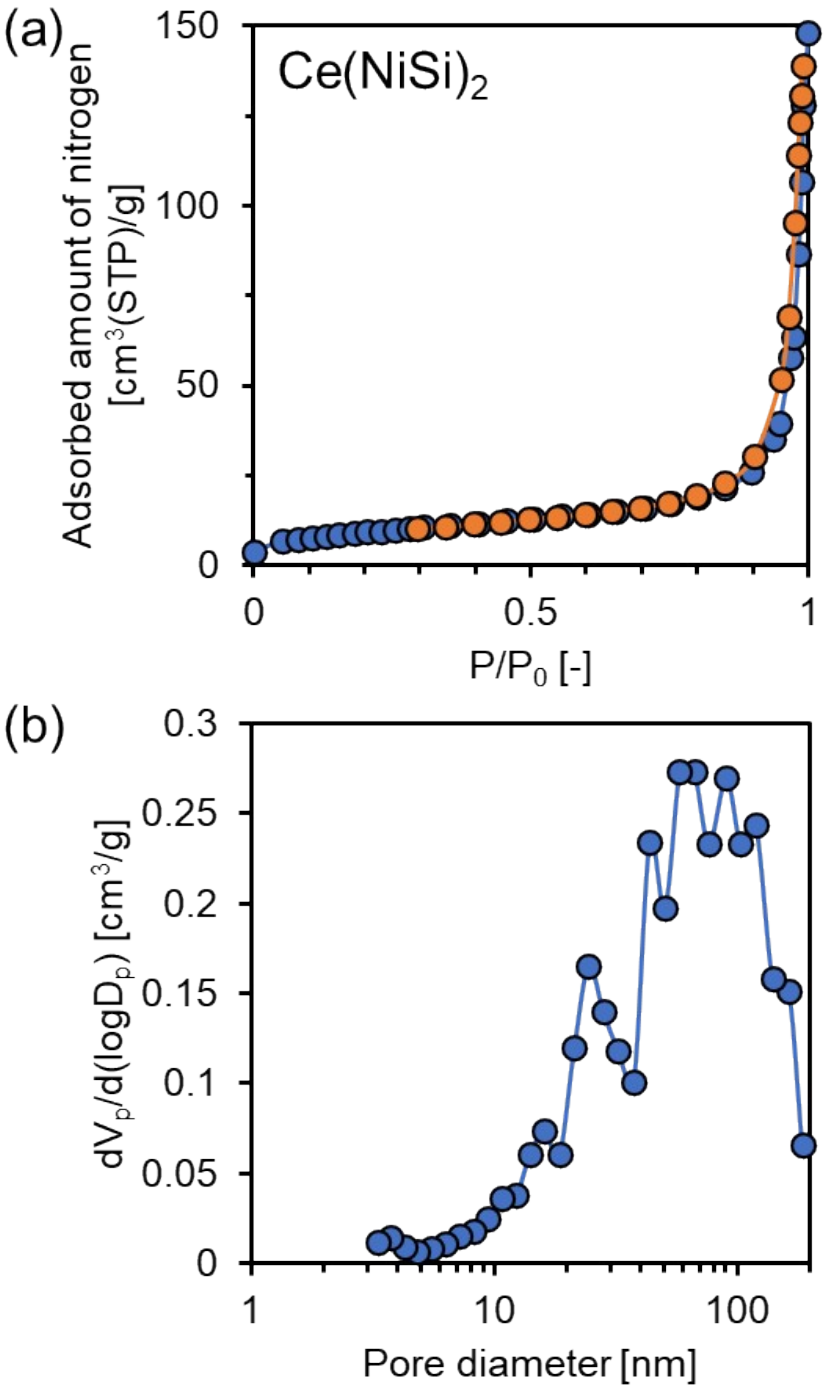

Fig. S8 (a) Adsorption (blue) and desorption (orange) isotherms of nitrogen, and (b) the corresponding pore size distribution for $Ce(NiSi)_2$.

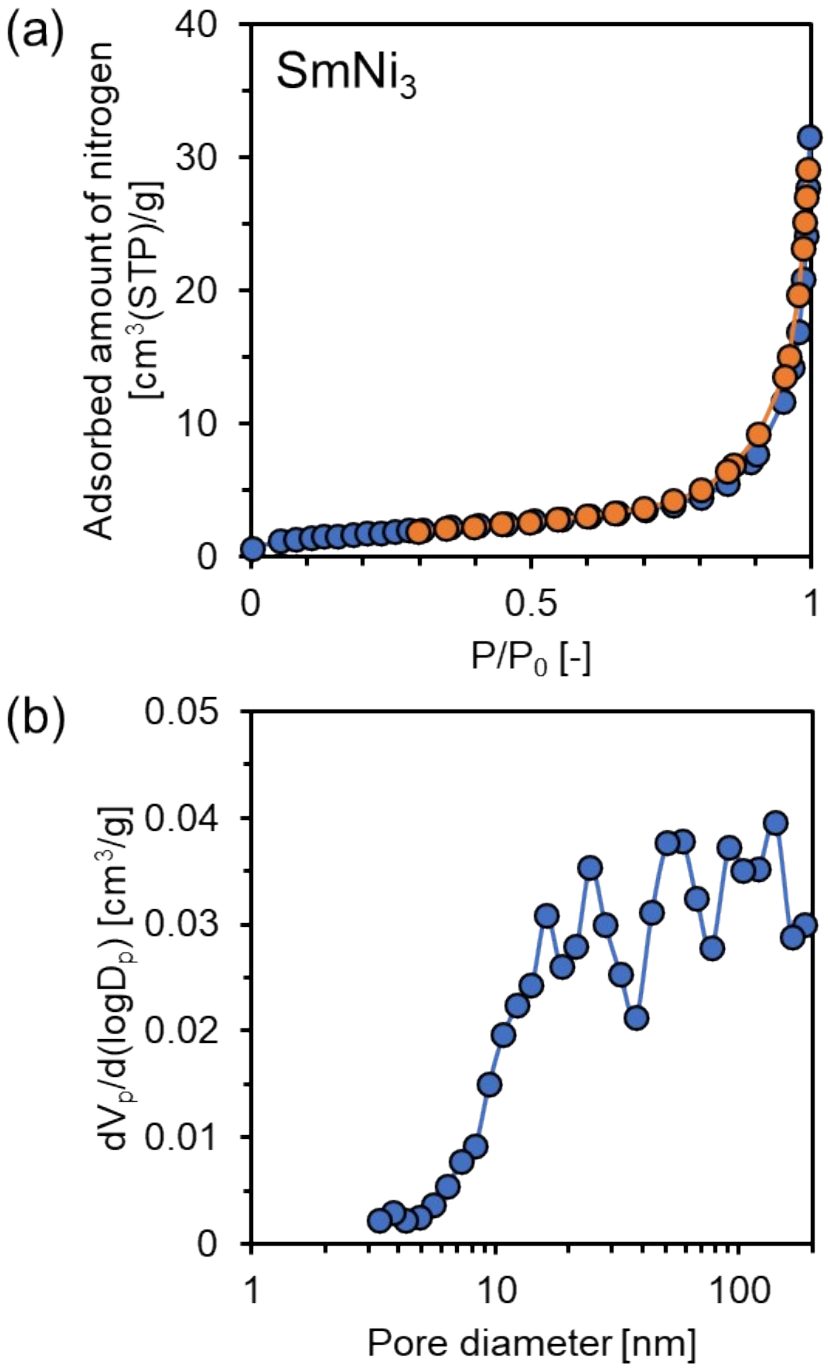

Fig. S9 (a) Adsorption (blue) and desorption (orange) isotherms of nitrogen, and (b) the corresponding pore size distribution for $SmNi_3$.

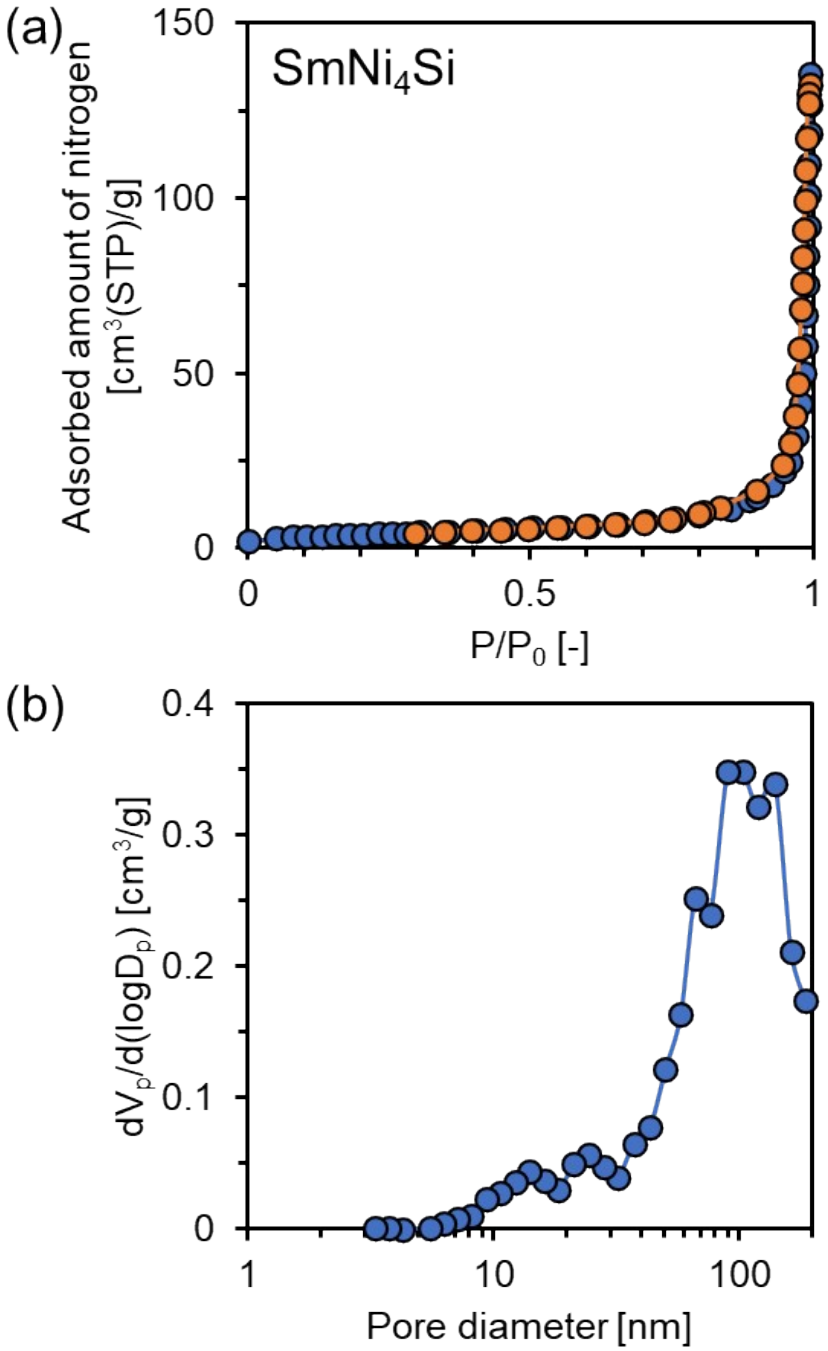

Fig. S10 (a) Adsorption (blue) and desorption (orange) isotherms of nitrogen, and (b) the corresponding pore size distribution for $SmNi_4Si$.

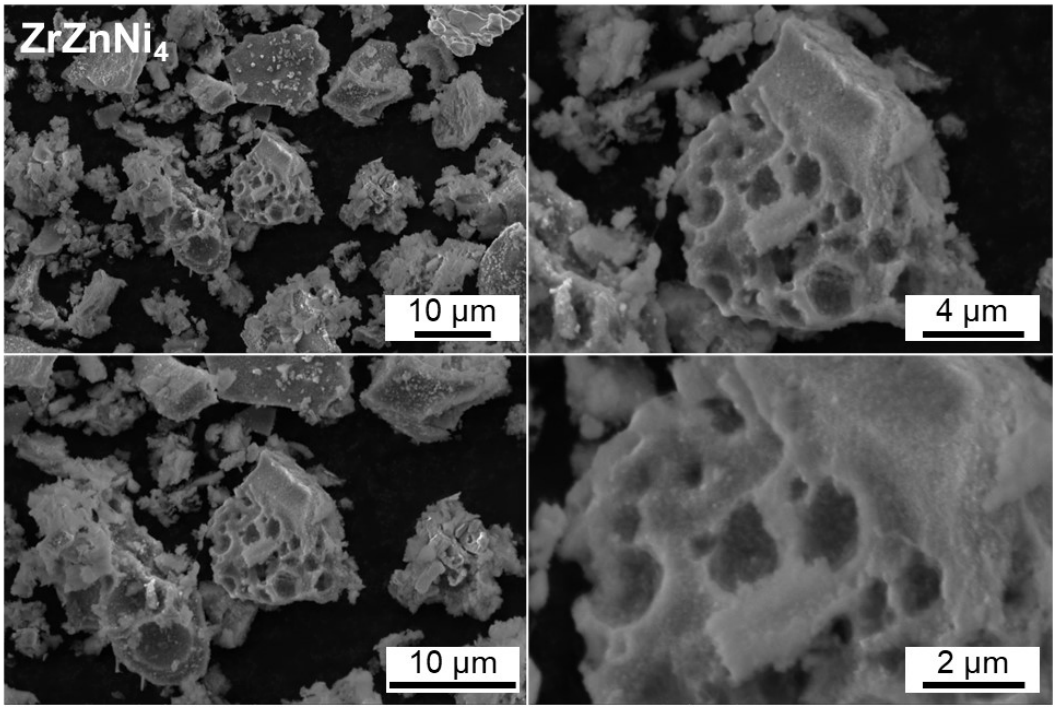

Fig. S11 SEM images for $ZrZnNi_4$.

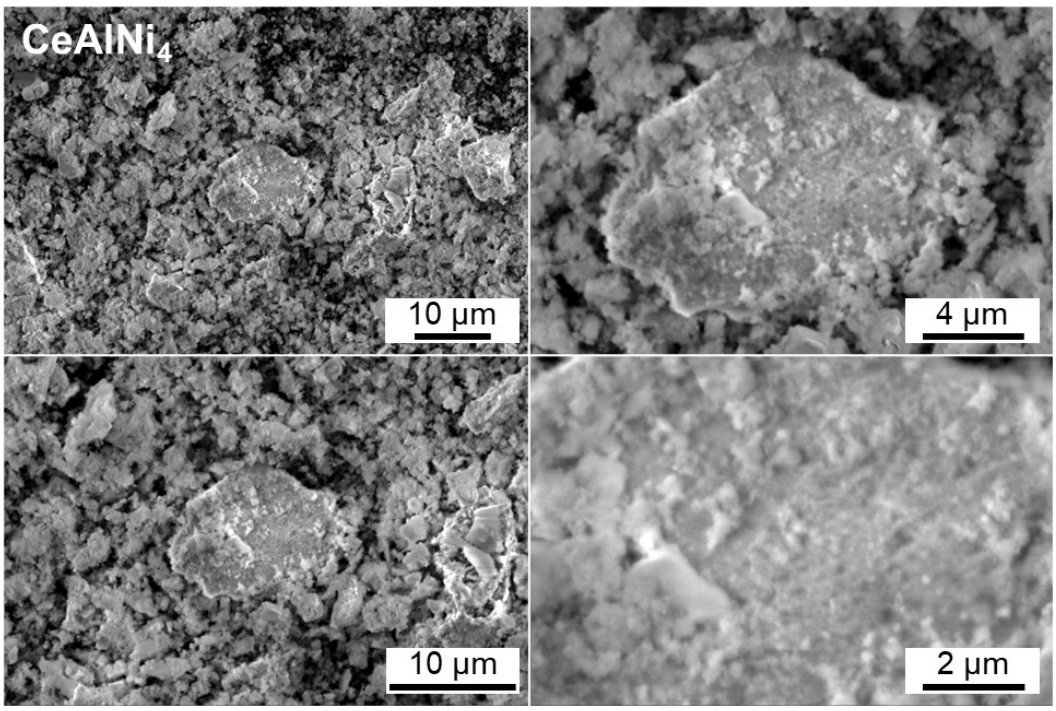

Fig. S12 SEM images for $CeAlNi_4$.

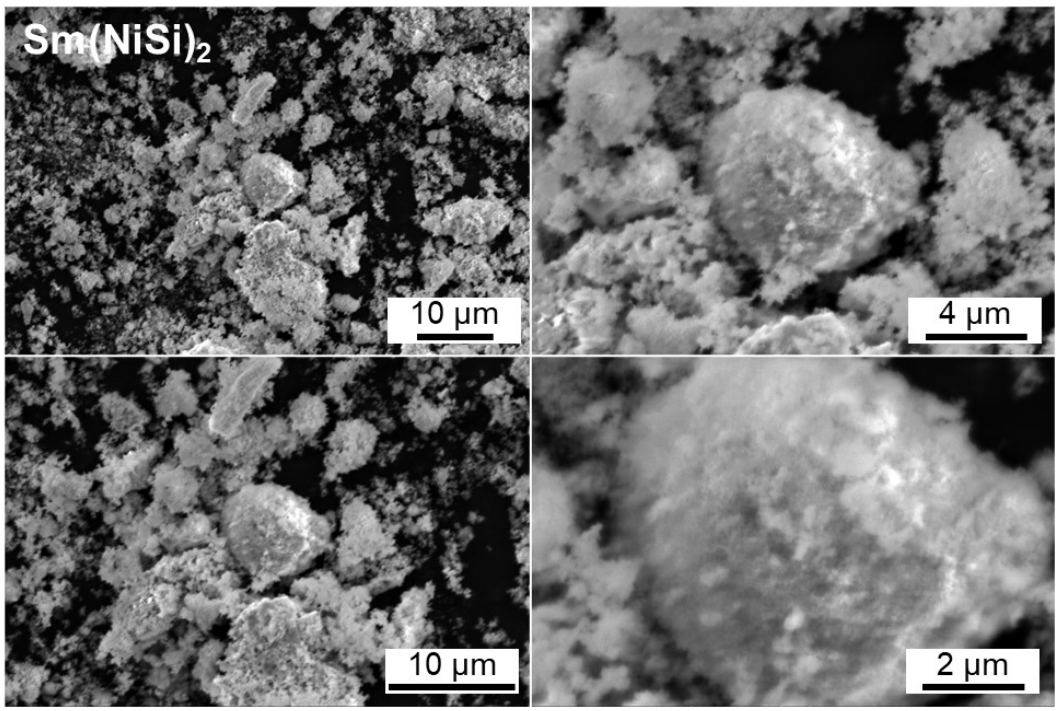

Fig. S13 SEM images for $Sm(NiSi)_2$.

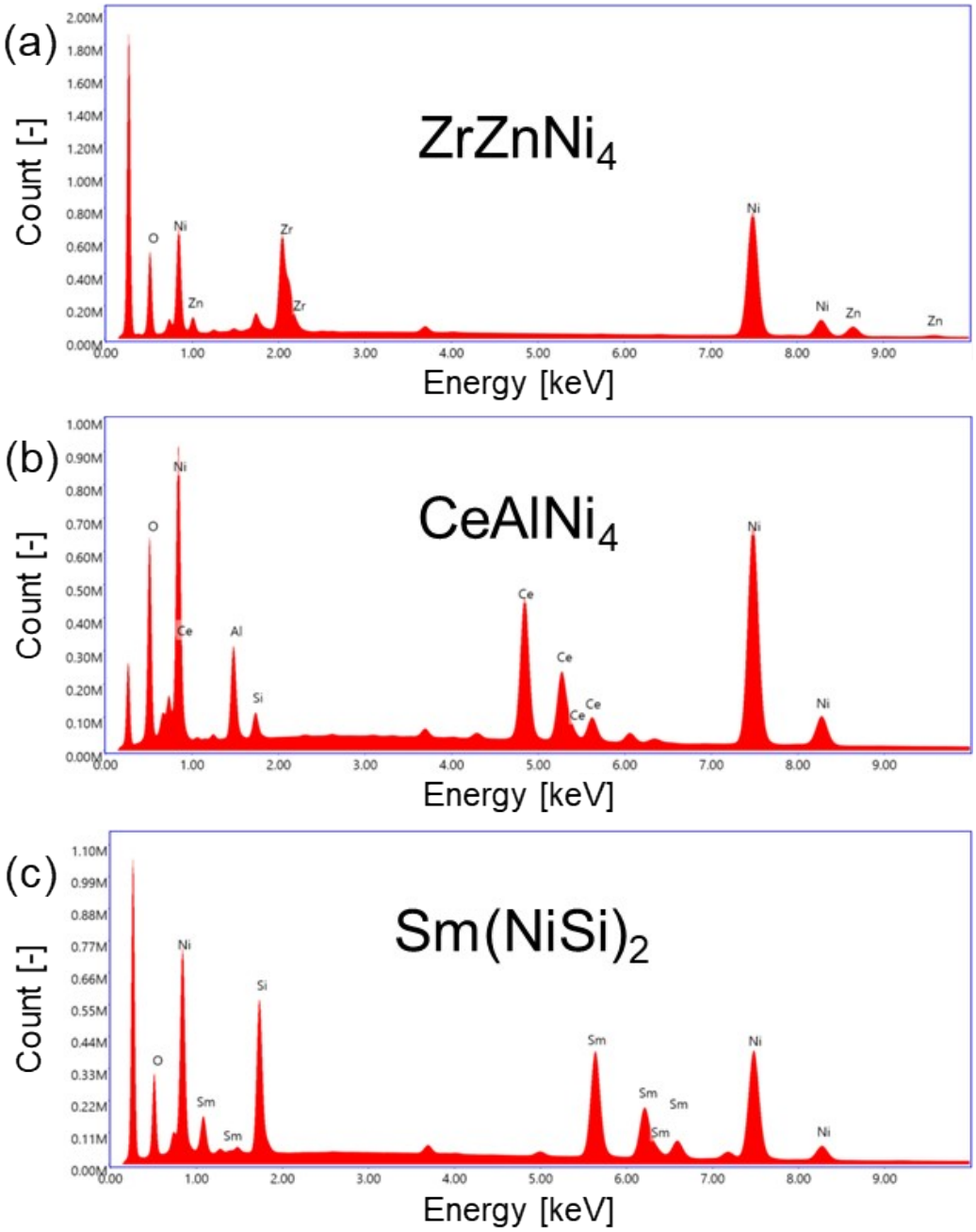

Fig. S14 EDX spectra obtained in SEM-EDX measurements for (a) $ZrZnNi_4$, (b) $CeAlNi_4$, and (c) $Sm(NiSi)_2$. The corresponding SEM images and elemental mappings are shown in Fig. 4.

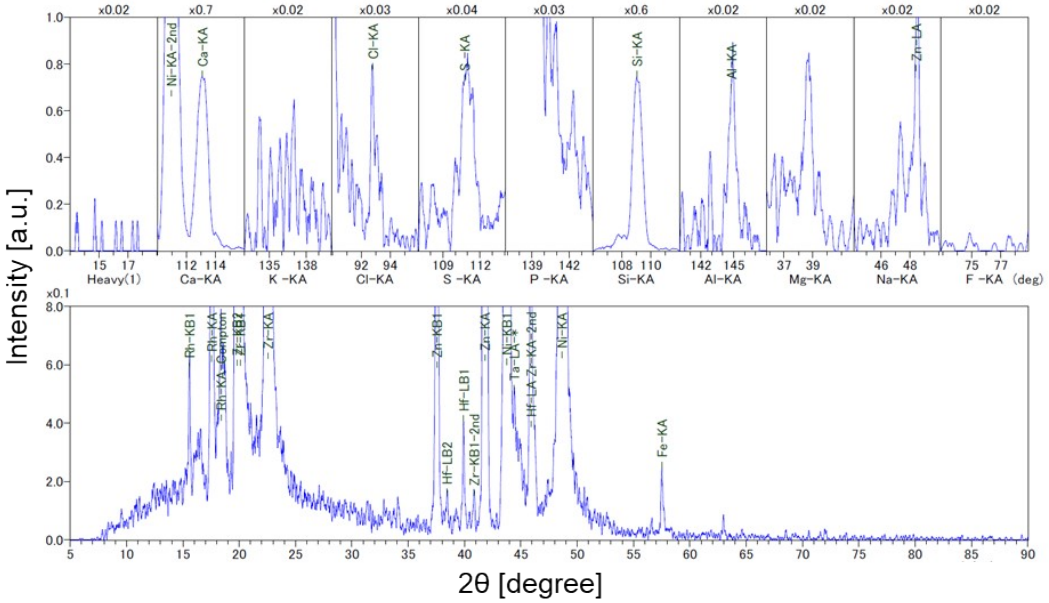

Fig. S15 XRF spectrum for $ZrZnNi_4$.

Table S1 The weight ratio and molar ratio of all the detected elements and ZrZn/Ni, respectively, in the XRF measurement for $ZrZnNi_4$.

Element	Mass%	Mol%
Zr	29.297	22.4
Zn	7.409	7.9
Ni	58.809	69.8
Si	2.073	-
Ca	1.095	-
Hf	0.983	-
Cl	0.125	-
Fe	0.117	-
Al	0.082	-
S	0.012	-

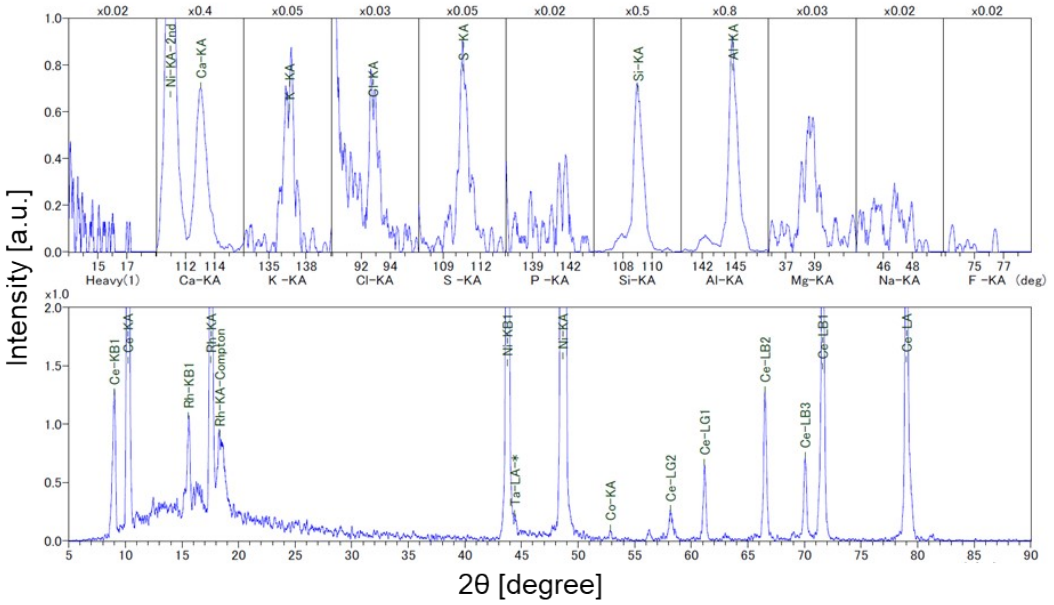

Fig. S16 XRF spectrum for $CeAlNi_4$.

Table S2 The weight ratio and molar ratio of all the detected elements and Ce/Al/Ni, respectively, in the XRF measurement for $CeAlNi_4$.

Element	Mass%	Mol%
Ce	36.436	18.6
Al	5.453	14.5
Ni	54.878	66.9
Si	2.239	-
Ca	0.612	-
Cl	0.108	-
Co	0.101	-
K	0.089	-
S	0.084	-

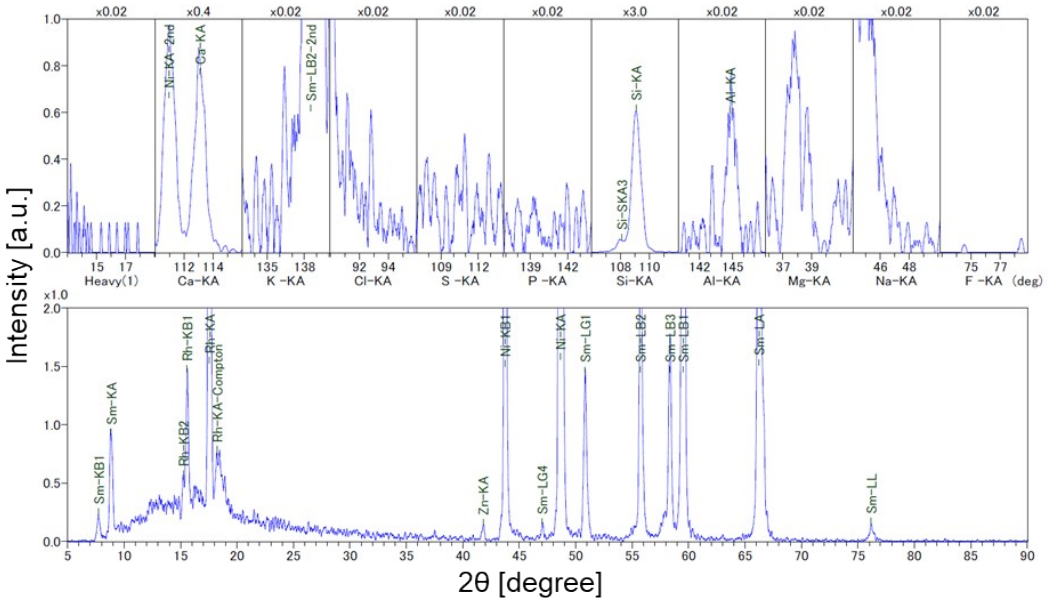

Fig. S17 XRF spectrum for $Sm(NiSi)_2$.

Table S3 The weight ratio and molar ratio of all the detected elements and Ce/Al/Ni, respectively, in the XRF measurement for $Sm(NiSi)_2$.

Element	Mass%	Mol%
Sm	51.306	24.8
Ni	35.667	44.1
Si	12.007	31.1
Ca	0.809	-
Zn	0.119	-
Al	0.093	-

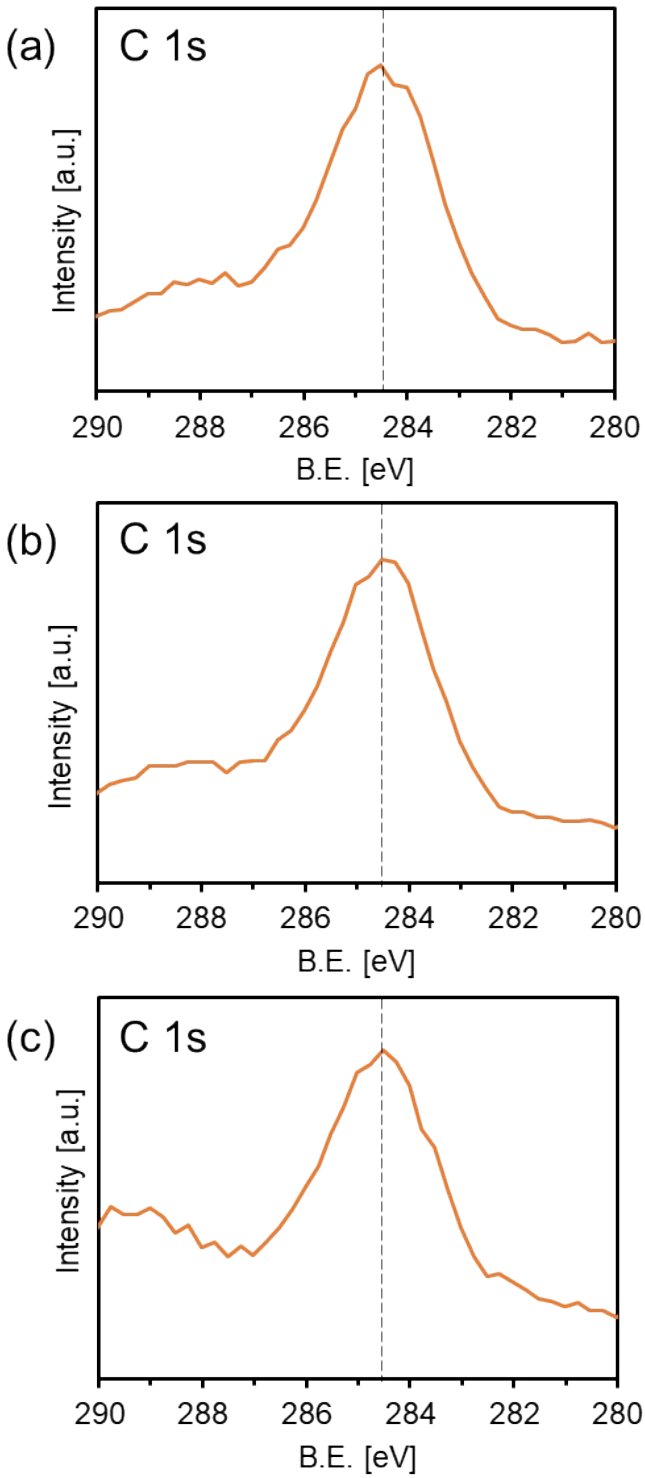

Fig. S18 XPS spectra of C 1s for (a) $ZrZnNi_4$, (b) $CeAlNi_4$, and (c) $Sm(NiSi)_2$.

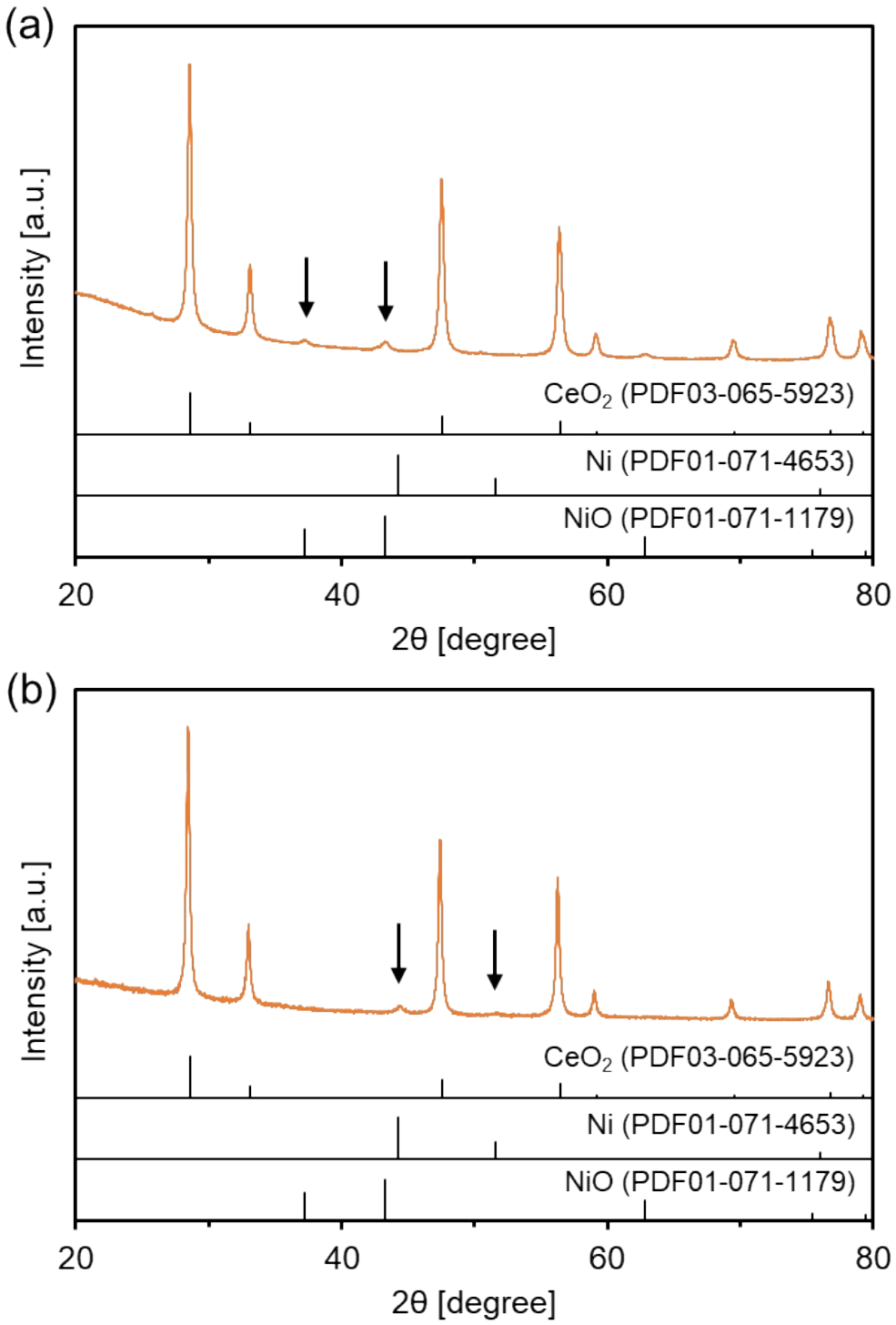

Fig. S19 XRD patterns for (a) 12wt%NiO/CeO_2 and (b) 10wt%Ni/CeO_2. Arrows indicates the main peak positions for NiO and Ni, respectively.